Multiphysics Modeling of Cellular Arrays Using Periodic Minimal Surfaces – A Drug and Gene Delivery Application

Jose I. Rey [1,2], Anthony J. Llewellyn[1,2], Andrew M. Hoff [1,3], Richard J. Connolly[1,2],
Jeffy P. Jimenez [1,2], Richard A. Gilbert[*,1,2]

[1] Center for Molecular Delivery, University of South Florida, Tampa, FL, USA,

[2] Department of Chemical and Biomedical Engineering, University of South Florida, Tampa, FL, USA,

[3] Department of Electrical Engineering, University of South Florida, Tampa, FL, USA

*Corresponding author: 4202 E. Fowler Ave. ENB-118. Tampa, FL 33620, gilbert@eng.usf.edu

Abstract: Minimal surfaces are found in nature from crystalline structures to biological nano and micro structures; such as biomembranes, and osseous formations in sea urchin. A model application to electrically mediated drug and gene delivery is presented. Periodic level surfaces which approximate minimal surfaces are used to generate a geometric representation of tissue. A method to create such structures in COMSOL Multiphysics using MATLAB functions is described.

Keywords: Drug and gene delivery, tissue geometry, minimal surface, DNA electrokinetics, tissue model, biophysical modeling, electroporation, iontophoresis.

1. Introduction

In vivo electroporation (EP) or electropermeabilization is a process that facilitates cellular uptake of a drug or gene by the application of short duration high voltage pulsed electric fields. The future clinical
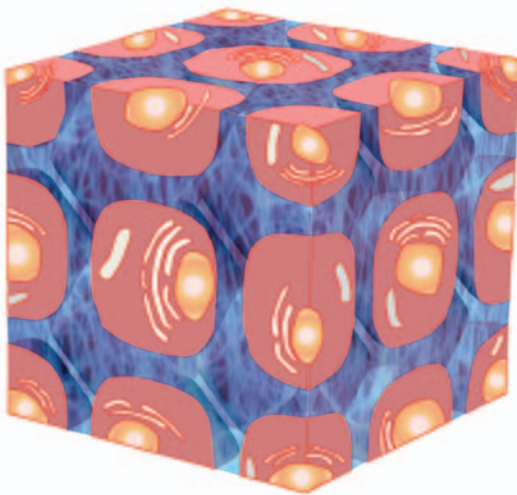
Figure 1. Representation of a tissue section with an array of cells containing nucli, organelles, and the interstitial space that fills the space between cells.

relevance of EP has been demonstrated in multiple clinical trials using chemotherapeutic agents [1, 2] and more recently, therapeutic genes [3]. The body of literature in the field cites many contributing factors to cause an increase in membrane permeability, such as the formation of transient nanopores and electrokinetic effects. Many models for EP have been developed; however, very few include geometry at the cell level in tissue matrixes.

Minimal surfaces are geometric conformations that result from optimization of physical properties of multiphase materials; these geometries are found in nature in a variety of structures and scales. They can be appreciated in non biological structures such as crystals, block co-polymers [4], soap films, and foams. Minimal surfaces are also present in biological structures at several scales, from cells, lipids organization in membranes and organelles[5] to osseous structures in sea urchin [6].

Triply periodic minimal surfaces can be approximated using Fourier expansions and level set surfaces composed of trigonometric functions [4]. The approach presented in this paper uses similar structures but modifies the continuity of such surfaces by including the absolute value function in the equality. The function used to describe cellular structures in this work is a modification of a surface belonging to the Neovius family of minimal surfaces, and takes the following form:

$$|\cos(2\pi x) + \cos(2\pi y) + \cos(2\pi z) \qquad (1)$$
$$+ \cos(2\pi x) \cos(2\pi y) \cos(2\pi z)| = s$$

where x, y and z represent Cartesian coordinates and s represents the level set cutting hyperplane.

These surfaces present a convenient way to model many systems including tissues with varied cell density, as cell density can be increased by approximating s to 0. This simple but powerful approach allows exploration of many tissue geometries by changing parameters defined in equation 1. Figure 1 shows a
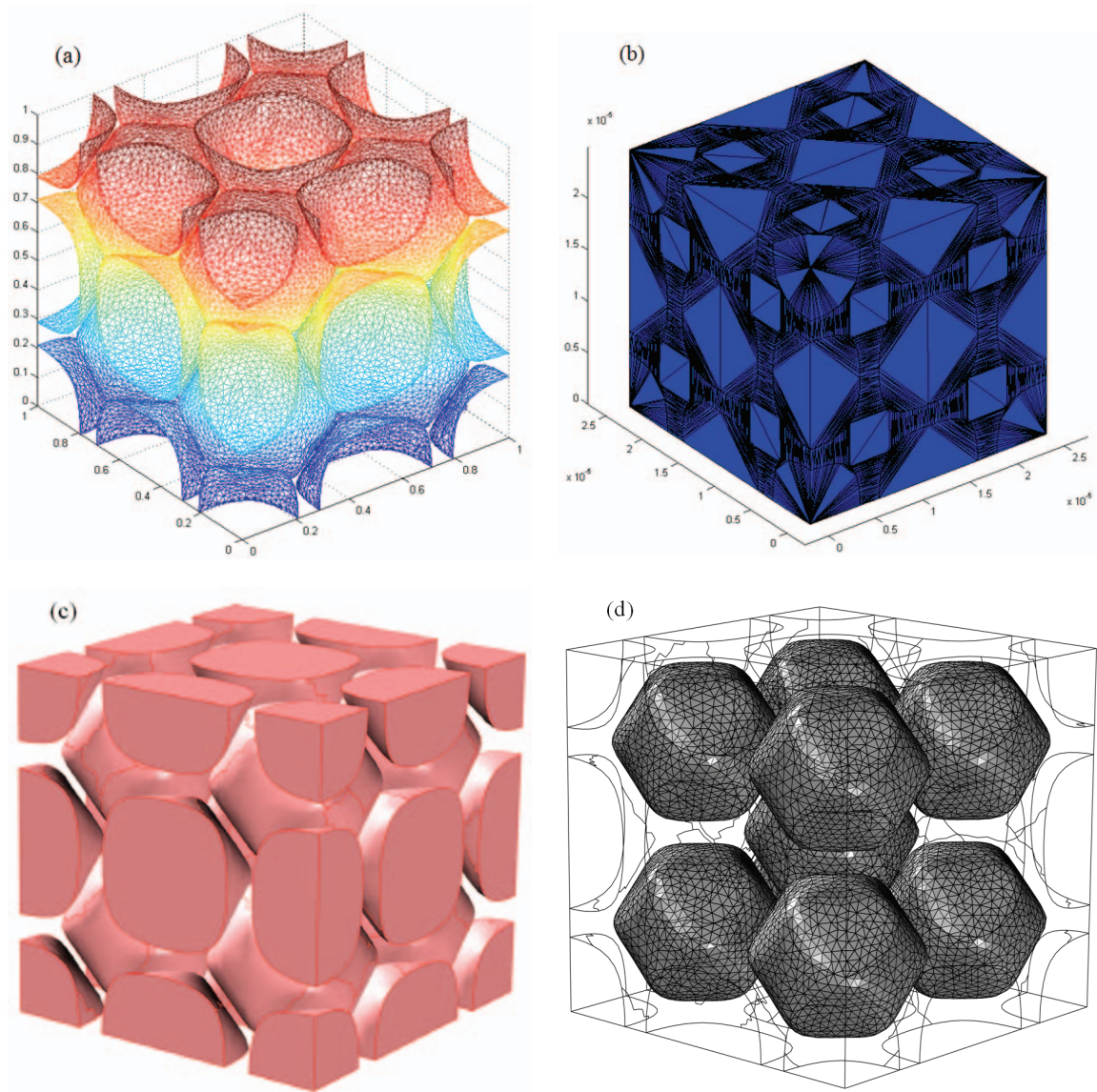
Figure 2. a) Simplified isosurface created in MATLAB, and simplified using CGAL and ISO2MESH scripts; b) Delaunay tessellation of simplified isosurface; c) Objects as imported to COMSOL Multiphysics; d) Final meshing using internal meshing.

representation of a tissue block that includes cells and the interstitial space between them. A higher cell density means the interstitial space is reduced.

The Center for Molecular Delivery at the University of South Florida has produced *in silico* tissues that mimic a variety of tissue types. To accomplish this, different matrix transformations have been applied to minimal surfaces to conform them to these tissue types.

2. *In Silico* Tissue Construction

The *in silico* tissue model was constructed using a variety of functions through MATLAB (The Mathworks, Inc.) scripting. First, a mesh of N^3 was created to describe the size of the tissue construct. Then the level surface function was evaluated using the built-in isosurface function. The resulting surface consisting of faces and vertices is then preconditioned using CGAL

(Computational Geometry Algorithms Library - cgal.org) MATLAB functions provided by ISO2MESH (iso2mesh.sourceforge.net) [7].

The preconditioned surface (Figure 2a) was converted to a minimal meshed volume (Figure 2b) using the Delaunay triangulation function, and imported into COMSOL Multiphysics (COMSOL AB) using the Femmesh and Geombject functions. Two subdomains were defined, one representing the cellular space (Figure 2c), and the other representing the filling interstitial space. The resulting geometry was then meshed using the internal COMSOL Multiphysics meshing algorithm.

3. DNA Electro Osmotic Transport in Tissue Block

The model presented here studies a particular physical aspect of electrically facilitated plasmid DNA delivery to cells. This model is intended to explore the electrokinetic events leading to plasmid DNA (pDNA) delivery into cells. To this end, some conditions were established prior to the selection of the mathematical model. First, the distribution of pDNA concentration in the interstitial space of the tissue construct resulting from an injection is assumed to be uniform. Second, an applied electric field resembling those used for *in vivo* gene electroporation protocols [3] was used. Third, the model is a simplification of *in vivo* scenarios in that the geometry of the tissue does not change as a result of electromechanical and pressure effects.

The starting point of the Multiphysics model was representing the applied electroporation pulse on the tissue construct. The result of this first step provided the potential gradients needed to set the electro osmotic flow boundary condition at the cells surface. With this, the velocity field calculation of the flow through the interstitial space between cells was determined. Then, the resulting flow velocities in addition to electrophoretic and diffusion gradients were used to calculate DNA concentrations in the interstitial space of the tissue construct. EP pulses of different durations were assessed using pulse length as a varying solver parameter.

Equation systems and methodology used in this model closely resembles the "Electrokinetic Flow in a DNA Chip" and "Electro osmotic Flow in Porous Media" models from the COMSOL Multiphysics Chemical Engineering modeling documentation [8].

3.1 Electric Field Distribution

The conductive media application mode was used to model the potential and current distribution in the tissue block using the Laplace equation on the point form of Ohm's law:
$$\nabla \cdot (-\sigma \nabla V) = 0 \qquad (2)$$
where ∇V [V/m] is the electric field intensity, and σ [S/m] is the electric conductivity.

Boundary conditions at the cell membranes were modeled as a current continuity:
$$\boldsymbol{n} \cdot (\mathbf{J}_1 - \mathbf{J}_2) = 0 \qquad (3)$$
where J_n [A/m^2] represent the current density vectors at the boundaries.

A potential difference yielding a field of 100 V/cm was applied across the tissue block using the boundary conditions.
$$V = V_0 \qquad (4)$$
where V_0 values are the potential at the boundaries.

Other tissue block exterior boundaries were modeled using the electric insulation boundary condition:
$$\mathbf{n} \cdot \mathbf{J} = 0 \qquad (5)$$

3.2 Electro Osmotic Flow

Navier-Stokes mode was used to solve the flow using the simplified equations for momentum transport and continuity in incompressible fluids:
$$\rho \frac{\partial \mathbf{u}}{\partial t} + \rho (\mathbf{u} \cdot \nabla)\mathbf{u} = \nabla \cdot [-p\mathbf{I} \qquad (6)$$
$$- \eta(\nabla \mathbf{u} + (\nabla \mathbf{u})^T)]$$
$$\nabla \cdot \boldsymbol{u} = 0 \qquad (7)$$
where $\mathbf{u}$ [m/s] is the velocity field vector, ρ [g/m^3] is the density of the fluid, $\mathbf{I}$ is the unity tensor, and η [Pa·s] is the dynamic viscosity of the fluid containing the pDNA.

The velocity at the cells surface is defined by the expression of electro osmotic induced velocities. The boundary condition at the surface of all cells was:
$$\mathbf{u}_0 = \frac{\varepsilon_{sol}\zeta}{\eta} \nabla V \qquad (8)$$
where ε_{sol} [F/m] is the electrical permittivity of the DNA solution, and ζ [V] is the zeta potential at the cell surface.
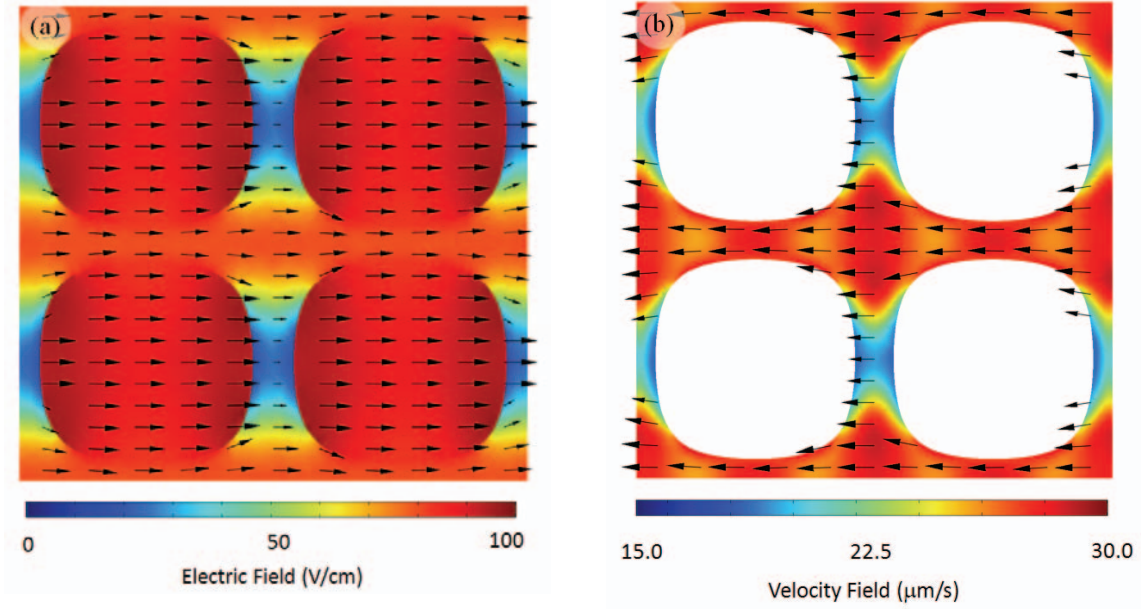
Figure 3. a) Electric field distribution through plane cutting four cells, arrows point in the direction of the resulting electric field distribution; b) Velocity field resulting from electro osmotic flow; arrows point in the direction of the induced flow at the cutting plane. Units for **E** [V/cm] and **u** [μm/s] have been adapted to agree with those used in drug and gene delivery literature.

The boundary condition is defined as a no viscous stress condition establishing the inlet and outlet at the exterior of the tissue block is:

$$\eta(\nabla\mathbf{u} + (\nabla\mathbf{u})^T) \cdot \mathbf{n} = 0 \qquad (9)$$

At all other faces of the tissue block the symmetry boundary condition was used:

$$\mathbf{n} \cdot \mathbf{u} = 0 \qquad (10)$$

3.3 Mass Transport of DNA

The mass transport for the DNA within the interstitial space is determined by the equation:

$$\frac{\partial c}{\partial t} + \nabla \cdot \mathbf{N} = 0 \qquad (11)$$

N denotes the flux vector [mol/(m^{2}s)] defined by the Nernst-Planck equation:

$$\mathbf{N} = -D\nabla c - zu_mFc\nabla V + c\mathbf{u} \qquad (12)$$

where the first term denotes the diffusivity of the species and encompasses D [m^2/s] which is the diffusion of DNA in the interstitial space, and c [mol/m^3] which is the concentration of DNA. The second term denotes electrophoretic drag, and is composed of the specie's charge number z, the mobility u_m, the Faraday constant, F [C/mol]. The third term denotes the convective flow that transports the concentration using the field velocity vector of the flow.

The mobility of the DNA is given by the Nernst-Einstein equation:

$$u_m = \frac{D}{RT} \qquad (13)$$

where R [J/mol·K] is the gas constant and T [K] is the temperature.

The boundary conditions at the inlet of the tissue construct maintain an unlimited supply of DNA:

$$c = c_0 \qquad (14)$$

The boundary condition at the outlet is convective flow represented by the equation:

$$\mathbf{n} \cdot (-D\nabla c - zu_mFc\nabla V) = 0 \qquad (15)$$

The rest of the exterior boundaries, and the boundaries defining the cell membrane are insulation/symmetry conditions:

$$\mathbf{n} \cdot \mathbf{N} = 0 \qquad (16)$$

4. Results

The solution of the DC conductive media problem yielded electric field intensities $|\nabla V|$ that ranged from 20 V/cm to 110 V/cm. Figure 3a shows distribution of such fields through a plane cutting 4 cells. Due to the low conductivity of the cells in comparison to that of the interstitial space, field lines traveling through the interstitial space are steered around cells to a certain degree.
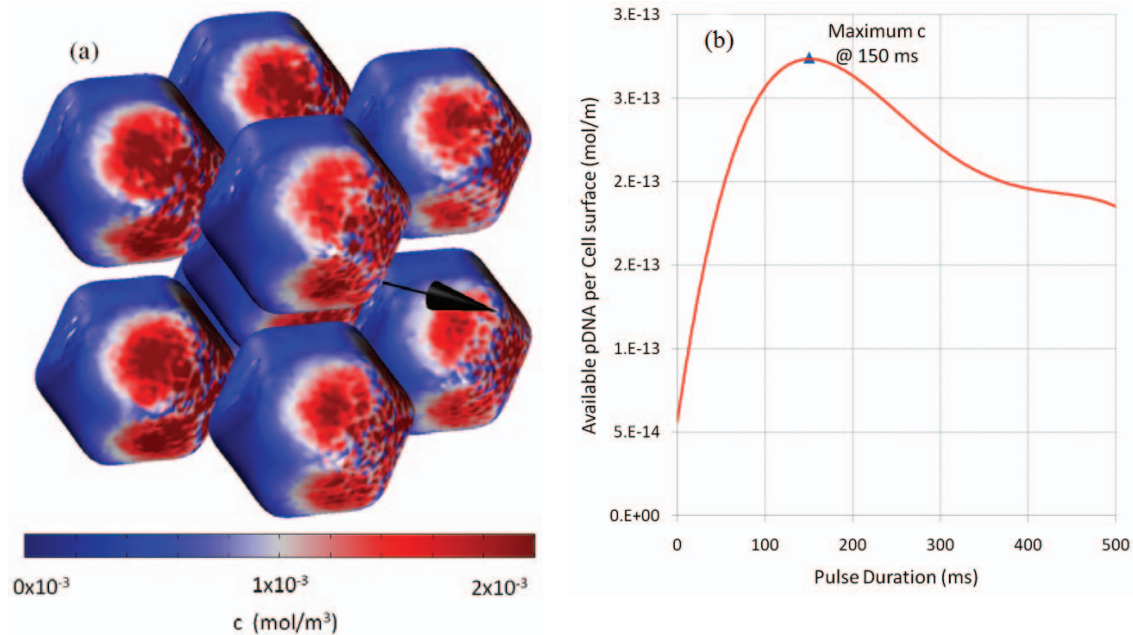
Figure 4. a) Available concentration at boundaries in mol/m^3 shows accumulation of DNA at the cell wals; single large arrow shows direction of electric field; b) Average integrated concentration at cells provides a time dependent concentration profile available to the cell; shows a maximum for a 150 ms pulse.

The solution to non compressible flow Navier-Stokes problem produced velocity fields that have direction close to 180° of that of electric field lines. The flow velocity field intensity varied from 15 μm/s to 30 μm/s (see Figure 3b). This represents roughly DNA electromobility of 1.5 to 3.0 μm for a 100 ms pulse. This value is within an order of magnitude of *ex vivo* experimental results presented by Zhaharoff et al [9].

The solution of the mass transport problem produced concentrations of DNA that were roughly 10 times higher than the original concentration ($2 \cdot 10^{-3}$ mol/m^3 compared to $1.71 \cdot 10^{-4}$ mol/m^3 initial concentration). The highest concentrations are present at the cell membrane portion of the cells that faces the convective flow of DNA opposing the direction of the applied electric field (see Figure 4a). This results in an increased concentration of DNA that seems to qualitative resemble that of direct visualizations of fluorescent DNA electroporated *in vitro* by Golzio, Teissie, and Rols [10] and Wasungu et al[11].

Figure 4b represents available concentration of DNA to a cell calculated as the average surface integral of concentrations at cell boundaries. The value for available DNA increases, reaching the maximum at 150 ms pulse length, followed by a decrease for the remainder of the pulse (500 ms in this case). This time dependence of available plasmid DNA to a cell provides a possible explanation for marginal benefit found for pulses longer than 150 ms for *in vivo* electroporation protocols that use similar applied electric fields [12].

5. Discussion and Conclusions

The current study showcases a geometrical platform for modeling processes that require periodic cellular structures in a continuous manner. A simple implementation of such parametric cellular structures was used to elucidate mechanisms of drug and gene delivery. Such implementation required the full use of geometric features conferred by the tissue construct. This approach provides an alternative to many other tissue geometrical approaches used to model normal and tumor tissue, such as those used in cellular automata, particle-based models, cellular potts, the immersed boundary model (IBcell) [13], and tissue templates[14].

The use of the proposed geometric building methods result in a very diverse groups of geometries that not only resemble tissues, but also foams, crystals and other naturally occurring geometrical objects. The ability to apply multiphysics modeling to such geometries provides a parametric framework that is also applicable to other physical phenomena. The Center for Molecular Delivery at the University of South Florida is currently using such geometries to extend investigation of other biophysical models[15] in cells to tissue constructs.

6. Acknowledgements

7. References

[1] M. Belehradek*, et al.*, "Electrochemotherapy, a new antitumor treatment. First clinical phase I-II trial," *Cancer,* vol. 72, pp. 3694-3700, 1993.

[2] L. F. Glass*, et al.*, "Intralesional bleomycin-mediated electrochemotherapy in 20 patients with basal cell carcinoma," *Journal of the American Academy of Dermatology,* vol. 37, pp. 596-599, 1997.

[3] A. I. Daud*, et al.*, "Phase I Trial of Interleukin-12 Plasmid Electroporation in Patients With Metastatic Melanoma," *J Clin Oncol,* vol. 26, pp. 5896-5903, December 20, 2008 2008.

[4] M. Wohlgemuth*, et al.*, "Triply Periodic Bicontinuous Cubic Microdomain Morphologies by Symmetries," *Macromolecules,* vol. 34, pp. 6083-6089, 2001.

[5] M. L. Lynch and P. T. Spicer, *Bicontinuous liquid crystals* vol. 127: CRC Press, 2005.

[6] G. Donnay and D. L. Pawson, "X-ray Diffraction Studies of Echinoderm Plates," *Science,* vol. 166, pp. 1147-1150, 1969.

[7] Q. Fang and D. A. Boas, "Tetrahedral mesh generation from volumetric binary and gray-scale images," 2009, pp. 1142-1145.

[8] Comsol AB, *COMSOL Multiphysics Chemical Engineering Module Model Library*, 2008.

[9] D. A. Zharoff*, et al.*, "Electromobility of plasmid DNA in tumor tissues during electric field-mediated gene delivery," *Gene therapy,* vol. 9, p. 19, 2002.

[10] M. Golzio*, et al.*, "Direct visualization at the single-cell level of electrically mediated gene delivery," *Proceedings of the National Academy of Sciences of the United States of America,* vol. 99, pp. 1292-1297, February 5, 2002 2002.

[11] L. Wasungu*, et al.*, "A 3D in vitro spheroid model as a way to study the mechanisms of electroporation," *International journal of pharmaceutics,* vol. 379, pp. 278-284, 2009.

[12] L. Heller*, et al.*, "Optimization of cutaneous electrically mediated plasmid DNA delivery using novel electrode," *Gene therapy,* vol. 14, pp. 275-280, 2006.

[13] K. A. Rejniak and L. J. McCawley, "Current trends in mathematical modeling of tumor-microenvironment interactions: a survey of tools and applications," *Experimental Biology and Medicine,* vol. 235, p. 411, 2010.

[14] S. Rajagopalan and R. Robb, "Cosmology inspired design of biomimetic tissue engineering templates with Gaussian random fields," *Medical Image Computing and Computer-Assisted Intervention–MICCAI 2006,* pp. 544-552, 2006.

[15] J. I. Rey*, et al.*, "Electrostrictive forces on vesicles with compartmentalized permittivity and conductivity conditions," *IEEE Transactions on Dielectrics and Electrical Insulation,* vol. 16, pp. 1280-1287, 2009.